

# SCIENTIFIC REPORTS



OPEN

## Refinement and growth enhancement of $\text{Al}_2\text{Cu}$ phase during magnetic field assisting directional solidification of hypereutectic Al-Cu alloy

Received: 22 December 2015

Accepted: 29 March 2016

Published: 19 April 2016

Jiang Wang<sup>1</sup>, Sheng Yue<sup>2</sup>, Yves Fautrelle<sup>3</sup>, Peter D. Lee<sup>2</sup>, Xi Li<sup>1</sup>, Yunbo Zhong<sup>1</sup> & Zhongming Ren<sup>1</sup>

Understanding how the magnetic fields affect the formation of reinforced phase during solidification is crucial to tailor the structure and therefore the performance of metal matrix *in situ* composites. In this study, a hypereutectic Al-40 wt.%Cu alloy has been directionally solidified under various axial magnetic fields and the morphology of  $\text{Al}_2\text{Cu}$  phase was quantified in 3D by means of high resolution synchrotron X-ray tomography. With rising magnetic fields, both increase of  $\text{Al}_2\text{Cu}$  phase's total volume and decrease of each column's transverse section area were found. These results respectively indicate the growth enhancement and refinement of the primary  $\text{Al}_2\text{Cu}$  phase in the magnetic field assisting directional solidification. The thermoelectric magnetic forces (TEMF) causing torque and dislocation multiplication in the faceted primary phases were thought dedicate to respectively the refinement and growth enhancement. To verify this, a real structure based 3D simulation of TEMF in  $\text{Al}_2\text{Cu}$  column was carried out, and the dislocations in the  $\text{Al}_2\text{Cu}$  phase obtained without and with a 10T high magnetic field were analysed by the transmission electron microscope.

Hypereutectic Al-Cu alloy is an ideal candidate for producing *in situ* composites because the multiphase structure that reinforced phases ( $\theta$ - $\text{Al}_2\text{Cu}$  phase) embedded in a flexible matrix (Al- $\text{Al}_2\text{Cu}$  eutectic phase) can be directly achieved by casting<sup>1</sup>. How to optimize the microstructure of hypereutectic alloy attracts long-term attentions because the performance of composites can be further tailored by modifying multiphase's microstructure such as the morphology of reinforced phases<sup>2</sup>. Implementing solidification control has been regarded as an efficient approach to achieve the microstructure optimization<sup>3</sup>, thus how to modify the solid structure of hypereutectic Al-Cu alloy via solidification control is worthy to study.

Applying magnetic field as an efficient solidification control method has been proposed more than half century ago<sup>4</sup> and was firstly introduced to metallurgy with the purpose of damping the melt flow<sup>5</sup>. Over half century's researches, the influence of magnetic field has been investigated on a wide range of metallic materials such as the pure metal<sup>6</sup>, single phase alloy<sup>7</sup>, monotectic alloy<sup>8</sup> and the eutectic alloy<sup>9</sup>. These studies have uncovered several effects of magnetic field other than damping flows, for instance changing both the liquid-to-solid and solid-to-solid phase transition temperature<sup>10,11</sup>, redistributing the primary phase, inclusions and the solute<sup>12,13</sup>, and aligning the grain/crystal orientation<sup>14</sup>. However, little attention has been paid to its impacts on solidification of the near-eutectic alloys (hypo- or hyper-eutectic alloys), in particular on the formation of primary reinforced phases. Although a few works can be found<sup>15,16</sup>, including our previous ones<sup>17,18</sup>, these studies mostly focus on how the magnetic field affect the orientation of primary phase in near-eutectic alloys or the orientation relationship between two phases of the eutectic alloys.

<sup>1</sup>State Key Laboratory of Advanced Special Steel, Shanghai University, Shanghai 200072, China. <sup>2</sup>The School of Materials, The University of Manchester, Oxford Road, Manchester, M13 9PL, UK. <sup>3</sup>SIMAP/EPM 1130 rue de la Piscine BP 75 ENSEEG, 38402 St-Martin d'Heres Cedex, France. Correspondence and requests for materials should be addressed to J.W. (email: wangjiang417@163.com) or Y.B.Z. (email: yunboz@staff.shu.edu.cn)

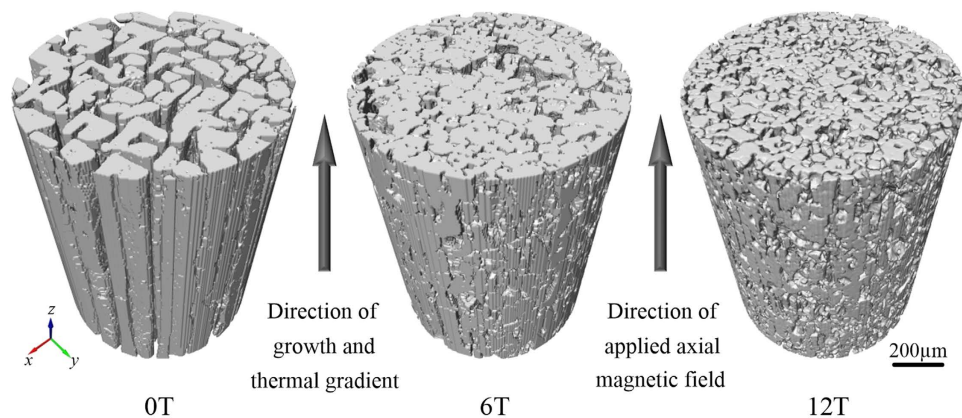


**Figure 1.** 3D morphology of primary  $\text{Al}_2\text{Cu}$  column solidified under different magnetic field flux intensities at the growth rate of  $2\ \mu\text{m/s}$  and thermal gradient of  $6000\ \text{K/m}$ .

Recently, a novel phenomenon that interaction between the thermoelectric currents and the applied magnetic field has been uncovered in the magnetic field assisting directional solidification of metals<sup>19,20</sup>. This interaction produces a kind of Lorentz forces that named thermoelectric magnetic forces (TEMF) because of its origins, and such forces exists in both solid and liquid phases<sup>21</sup>. TEMF in liquid can generate flow ahead of the solid/liquid interface<sup>19</sup>. This is contrary to the previous knowing that the uniform static magnetic field can only damp the melt flow, and thus drawn a huge of attentions<sup>22–24</sup>. Nevertheless, rare work has been done on understanding the influence of TEMF in the solid, and in particular its impact on the formation of primary reinforced phase during solidifying the metal matrix *in situ* composites.

Considering so, the hypereutectic Al-40 wt.%Cu alloys were directional solidified under different axial magnetic fields and the solidification structure was quantified in 3D using high resolution synchrotron X-ray tomography. The experimental results show that the primary  $\text{Al}_2\text{Cu}$  phase was refined and its total volume was increased by the magnetic field. TEMF in the solid  $\text{Al}_2\text{Cu}$  column was simulated based on its real structure, and the computed results indicate a torque can form on the column due to the TEMF. This torque would fragment the continuously grown column and respond to the refinement. In another aspect, TEMF causing dislocation multiplication can facilitate the atom attachment during faceted phase growth, which may lead to the  $\text{Al}_2\text{Cu}$  phase's total volume increase that we call growth enhancement in the present report.

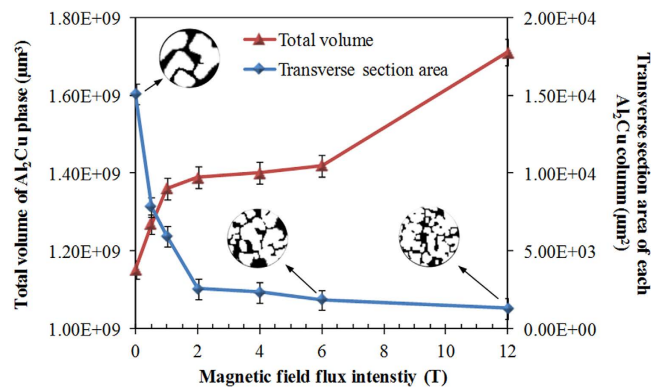
## Results

Figure 1 shows the 3D morphology of primary  $\text{Al}_2\text{Cu}$  columns achieved under axial magnetic fields of 0T, 6T and 12T respectively. The eutectic phases, which occupy the interspaces between columns, have been eliminated from the 3D view to expose the  $\text{Al}_2\text{Cu}$  phase. Without magnetic field, many typical  $90^\circ$  angles between faces of the columns indicate that these  $\text{Al}_2\text{Cu}$  phases are faceted, and it can see that these columns grow continuously in axial direction. The refinement of  $\text{Al}_2\text{Cu}$  column can be observed both in transverse and longitudinal sections of the sample obtained under a 6T axial magnetic field, and the decrease of interspaces between columns means the increase of  $\text{Al}_2\text{Cu}$  phase's total volume. Moreover, less  $90^\circ$  angle faces in the columns suggests that the faceted feature of the primary  $\text{Al}_2\text{Cu}$  phase tends to transform into a non-faceted appeal. By increasing the magnetic field to 12T, the degrees of refinement and growth enhancement further increase, and  $\text{Al}_2\text{Cu}$  phases' non-faceted feature become dominating.

To confirm and quantify the refinement and growth enhancement of  $\text{Al}_2\text{Cu}$  phase under magnetic field, the transverse section area of each column and their total volume were respectively calculated based on the 3D tomography data and plotted as a function of magnetic fields as shown in Fig. 2. It clearly shows that the total volume of primary  $\text{Al}_2\text{Cu}$  phase increase with the magnetic fields, and reversely the transverse section area of each column gradually decrease. The decreased area indicates the refinement of the  $\text{Al}_2\text{Cu}$  column. The 3D structure quantification shows that all the  $\text{Al}_2\text{Cu}$  columns contacting with each other, which is understandable because columns may contact during growth or initially grow from the same seed. This makes identifying a single  $\text{Al}_2\text{Cu}$  column difficult, and thus its transverse section area but not the volume was used to indicate the refinement effect. Better than cutting the sample into a number of slices and then measuring the transverse section area of columns in each slice to minimize the error, we can easily get sufficient slices using the tomography data. To more precise, the transverse section area of each  $\text{Al}_2\text{Cu}$  column in Fig. 2 was produced by averaging that from 60 slices over the sample.

## Discussions

The refinement of  $\text{Al}_2\text{Cu}$  column may attribute to its fragmentation<sup>21</sup> caused by the TEMF because the present solidification conditions permit the interaction between thermoelectric currents and magnetic field. The thermal gradient along solid-liquid interface together with the dissimilar thermo-physical properties (e.g. thermoelectric power) between solid and the melt give rise to the occurring of Seebeck effect, which results in thermoelectric currents flowing through both solid and melt<sup>25</sup>. To confirm this and understand how TEMF fragment the  $\text{Al}_2\text{Cu}$  column, a 3D simulation of TEMF was performed based on the real  $\text{Al}_2\text{Cu}$  structure that got from the tomography data and shown in Fig. 3(a). The detailed description of simulation method can be found in ref. 26 and the



**Figure 2.** Total volume of the Al<sub>2</sub>Cu phase and transverse section area of each Al<sub>2</sub>Cu column plotted as a function of applied magnetic field flux intensities.

related physical parameters of Al<sub>2</sub>Cu and the melt are listed in Table 1. The temperature field, electric current density and fluid flow field was coupled to simulate TEMF using a finite element method based commercial code COMSOL Multiphysics. Figure 3(b,c) respectively shows the  $x$  and  $y$  component magnitude of the computed TEMF in Al<sub>2</sub>Cu column under a 12T axial magnetic field. It can find that TEMF orientate anticlockwise at the top (hot region) and clockwise at the bottom (cool region), so that a torque as indicated by the black arrows in Fig. 3(a) forms on the column. As the Al<sub>2</sub>Cu always grows ahead the eutectic front, the excess part of Al<sub>2</sub>Cu column could be fractured by this torque. Considering so, the discontinuous growth of Al<sub>2</sub>Cu column in axial direction could form under magnetic field, and this is just the case indicated by Fig. 3(d) that the longitudinal structure of Al-40 wt.%Cu alloys fabricated without and with a 12T magnetic field. In fact, as reflected by Fig. 3(e), the decrease transverse section area of each column can be interpreted by the TEMF as well. Figure 3(f) is the distribution of computed total stress in Al<sub>2</sub>Cu column in a transverse ( $x-y$ ) plane at the column top. Subjecting to such stresses this column should tend to rotate, as mentioned above this column may contact with another one at any point around its edge during the rotation. Assuming this column contacts with and is blocked by the other one at the point marked by the black circle, it would not be difficult to image that the upper left part of this column would depart away under the stresses orienting towards to negative  $x$  axis. It is worthy to point out that the transverse section area of each Al<sub>2</sub>Cu column decrease gradually with magnetic fields is because the TEMF is linearly proportional to the applied magnetic field flux intensity<sup>21</sup>.

In terms of the increase of Al<sub>2</sub>Cu phases' total volume, which is attributed to the fasted growth rate of the faceted phases when magnetic field is presence. It is known that the faceted phase's growth rate is dominated by the atom attachment process, and the defects in the solid, like dislocations, could provide more vacancies for the approaching atoms to easy their locating. It is therefore not difficult to get that the dislocation multiplication could fast the growth of faceted phases. It is so happen that the stressed solid is a favourite condition for the dislocation multiplication, and thus the strong stresses (up to  $3.3 \times 10^8$  N/m<sup>2</sup>) caused by TEMF in the Al<sub>2</sub>Cu column are thought to be the main reason for the observed growth enhancement. To verify such interpretation, the dislocations in the solid were analysed by the transmission electron microscope. Figure 4 shows the bright field images of Al-40 wt.%Cu samples fabricated without and with a 10T magnetic field. It manifests that a number of dislocations form in the sample solidified under magnetic field and nearly dislocation free structure is obtained without the magnetic field. Moreover, it should point out that the continuous increase of Al<sub>2</sub>Cu columns' total volume with magnetic field can be also explained by the linear proportion of TEMF to the applied magnetic fields.

Additionally, except the dislocation multiplication, we would like to mention several other phenomena those may contribute to the primary Al<sub>2</sub>Cu phases' growth enhancement when the magnetic field is presence. In fact, the magnetic field induced change of phase transitions temperature<sup>10</sup>, and diffusion behaviour modification<sup>27</sup> may also affect the growth of Al<sub>2</sub>Cu phase. Upon the change of phase transition, our previous work<sup>28</sup> has been revealed that the magnetic field can increase the solidification undercooling of Al<sub>2</sub>Cu phase. The higher undercooling may lead to the faster growth rate and then increase the Al<sub>2</sub>Cu phases' total volume. The altered diffusion behaviour may also contribute to the growth enhancement because the solidified Al<sub>2</sub>Cu phases continue to growth through diffusion.

## Conclusions

In summary, morphology of the primary Al<sub>2</sub>Cu phase obtained under different axial magnetic fields has been quantified for the first time in 3D using high resolution synchrotron X-ray tomography. Both refinement and growth enhancement of the Al<sub>2</sub>Cu were observed and their degrees increase with the applied magnetic fields. TEMF in solid Al<sub>2</sub>Cu column were confirmed by carrying out a real structure based 3D simulation, and capable to produce a torque on the column. The refinement is therefore attributed to the fragmentation of Al<sub>2</sub>Cu column by the torque. TEMF in solid Al<sub>2</sub>Cu leading to the dislocation multiplication was proposed, and verified by the transmission electron microscope analysis. This may respond to growth enhancement of the faceted Al<sub>2</sub>Cu phase, because defects in the solid can facilitate the atom attachment and thus fast the Al<sub>2</sub>Cu phase's growth. The gradually increase degree of refinement and growth enhancement can be interpreted by the direct proportion between TEMF and the applied magnetic field flux intensity.



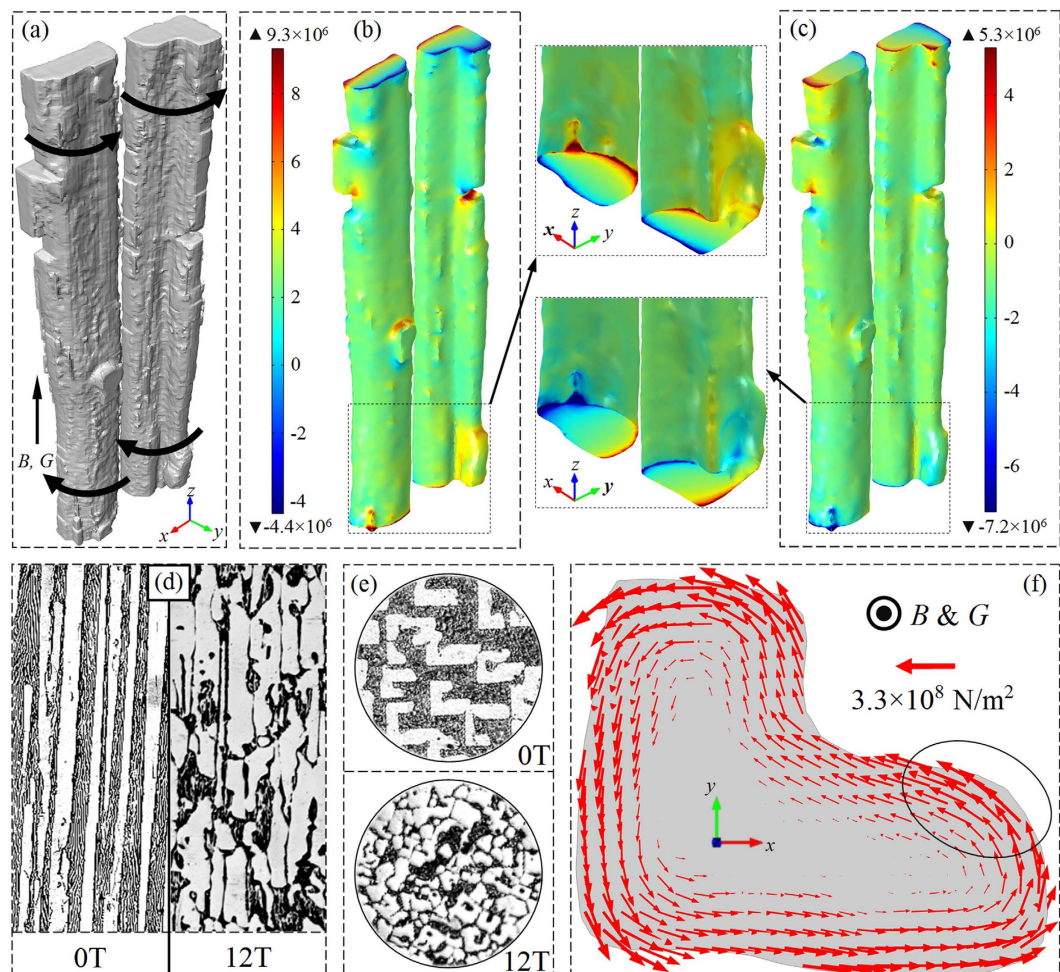


**Figure 3.** (a)  $\text{Al}_2\text{Cu}$  column obtained without magnetic field; (b) x component magnitude of computed thermoelectric magnetic forces (TEMF) in  $\text{Al}_2\text{Cu}$  column; (c) y component magnitude of computed TEMF in  $\text{Al}_2\text{Cu}$  column; (d) and (e) Longitudinal and transverse structure of Al-40 wt.%Cu alloys obtained without and with magnetic field at growth rate of  $2\ \mu\text{m/s}$ ; (f) Distribution of computed total stress in a transverse ( $x$ - $y$ ) plane at the column top. (For both experiment and simulation,  $B = 12\text{T}$  and  $G = 6000\ \text{K/m}$ , the unit of colour legend is  $\text{N/m}^3$ ).

Names and Units of the parameter	$\text{Al}_2\text{Cu}$	Melt
Electrical conductivity, $\Omega^{-1}\cdot\text{m}^{-1}$	$6.20 \times 10^6$	$3.05 \times 10^6$
Absolute thermoelectric power, $\text{V}\cdot\text{K}^{-1}$	$-0.60 \times 10^{-6}$	$-2.25 \times 10^{-6}$

**Table 1.** Physical parameters of  $\text{Al}_2\text{Cu}$  phase and melt used for the 3D simulation.

### Experimental Methods

The detailed experimental apparatus and process can be found in ref. 26. In brief, Al-40 wt.%Cu alloy was prepared with the high-purity Al and Cu elements by an argon gas (1 atm) filled induction furnace. The rod-like sample was 3 mm in diameter and 150 mm long, which was sealed in a corundum crucible with 3 mm inner diameter and 200 mm length. The directional solidification was upward and conducted by a Bridgman type furnace that was insulated from the Ga-In-Sn liquid metal pool by a refractory disc. The thermal gradient in the sample was controlled by adjusting the temperature of the furnace. The superconductor magnet supplied by Oxford Instrument Ltd. provided an axial magnetic field with adjustable intensity up to 14T. During the experiment, the sample within crucible was pulled down at a constant speed of  $2\ \mu\text{m/s}$  and an upward thermal gradient of  $6000\ \text{K/m}$ .

The high resolution synchrotron X-ray tomographic imaging of samples was carried out on Beamline I12 at the Diamond Light Source (DLS), Harwell, UK using a monochromatic beam of 53 KeV. The PCO.edge high resolution camera was used as the detector, and its pixel size is  $1.3 \times 1.3\ \mu\text{m}^2$ . The exposure time of 5 ms was chosen to guarantee the sufficient transmission and good contrast, the field of view is  $3.3 \times 2.8\ \text{mm}^2$  (number of

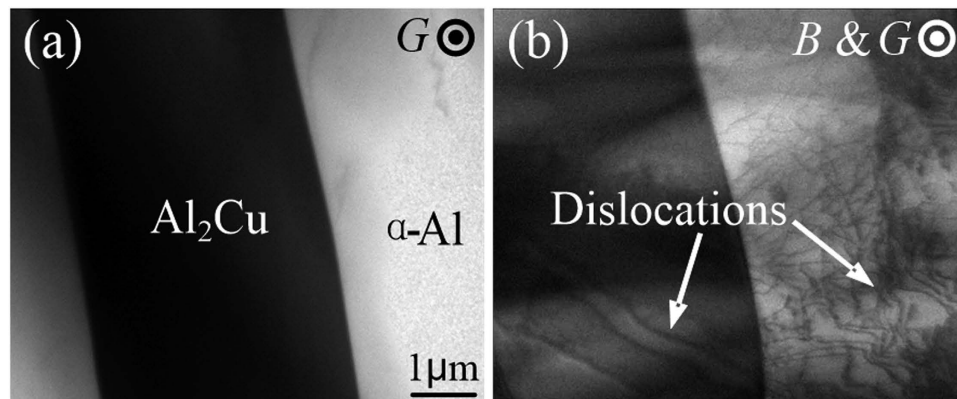


**Figure 4.** Bright field transmission electron microscope images of Al–40 wt.%Cu alloys obtained without (a) and with a 10T magnetic field (b) at the growth rate of 2  $\mu\text{m/s}$  and the thermal gradient of 6000 K/m.

pixels of each X-ray image: 2560  $\times$  2160 pixel), and 1800 frames were collected for one complete 3D tomography. Moreover, the detailed description of 3D tomography apparatus and reconstruction methods can be found in ref. 29. The volume data visualisation and quantification were carried out using Avizo 7 (Visualization Science Group, France) and Matlab (version 2012B with Image Processing Toolbox, Mathworks Inc., USA). The detail procedures have been described in ref 30, and the 3D renderings in this work were contoured at 40  $\text{cm}^{-1}$ .

## References

1. Bei, H., Pharr, G. M. & George, E. P. A review of directionally solidified intermetallic applications. *J. Mater. Sci.* **39**, 3975–3984 (2004).
2. Steen, H. A. H. & Hellawell, A. Structure and properties of aluminium-silicon eutectic alloys. *Acta Metal.* **20**, 363–370 (1972).
3. Yan, N., Geng, D. L., Hong, Z. Y. & Wei, B. Ultrasonic levitation processing and rapid eutectic solidification of liquid Al–Ge alloys. *J. Alloys Comp.* **607**, 258–263 (2014).
4. Youdelis, W. V., Colton, D. R. & Cahoon, J. On the theory of alloy solidification in a magnetic field. *Can. J. Phys.* **42**, 2238–2258 (1964).
5. Chedzey, H. A. & Hurlle, D. T. J. Avoidance of growth-striae in semiconductor and metal crystals grown by zone-melting techniques. *Nature* **210**, 933–934 (1966).
6. Vives, Ch & Perry, Ch. Solidification of a pure metal in the presence of a stationary magnetic field. *Int. Comm. Heat Mass Transfer* **13**, 253–263 (1986).
7. Liu, T. *et al.* Effects of high magnetic fields on the microstructures and grain boundaries in binary Al–Li alloy. *J. Alloys Comp.* **469**, 258–263 (2009).
8. Wang, J. *et al.* Influence of static high magnetic field on the liquid-liquid separation of hyper-monotectic alloy. *Appl. Phys. A* **112**, 1027–1031 (2013).
9. Li, X., Ren, Z. M. & Fautrelle, Y. Effect of high magnetic fields on the microstructure in directionally solidified Bi–Mn eutectic alloy. *J. Cryst. Growth* **299**, 41–47 (2007).
10. Perez-Landazabal, J. I., Recarte, V., Torrens-Serra, J. & Cesari, E. Relaxation effects in magnetic-field-induced martensitic transformation of an Ni–Mn–In–Co alloy. *Acta Mater.* **71**, 117–125 (2014).
11. Li, X., Ren, Z. M. & Fautrelle, Y. High-magnetic-field-induced solidification of diamagnetic Bi. *Scripta Mater.* **59**, 407–410 (2008).
12. Sun, Z., Guo, M. X., Vleugels, J., Van der Biest, O. & Blanpain, B. Strong magnetic field-induced segregation and alignment of nonmagnetic particles. *J. Appl. Phys.* **109**, 07E301 (2011).
13. Wang, Q. *et al.* A novel method for *in situ* formation of bulk layered composites with compositional gradients by magnetic field gradient. *Scripta Mater.* **56**, 1087–1090 (2007).
14. Deng, P. R. & Li, J. G. Slow cooling conditions for texturing ferromagnetic materials by solidification in a magnetic field. *Scripta Mater.* **55**, 747–750 (2006).
15. Kotadia, H. R. & Das, A. Modification of solidification microstructure in hypo- and hyper-eutectic Al–Si alloys under high-intensity ultrasonic irradiation. *J. Alloys Comp.* **620**, 1–4 (2015).
16. McKeown, J. T. *et al.* *In situ* transmission electron microscopy of crystal growth-mode transitions during rapid solidification of a hypoeutectic Al–Cu alloy. *Acta Mater.* **65**, 56–68 (2014).
17. Fan, D. D. *et al.* Effect of a transverse magnetic field on solidification structure in directionally solidified Sn–Pb hypoeutectic alloys. *J. Cryst. Growth* **402**, 319–324 (2014).
18. Li, X., Gagnoud, A., Fautrelle, Y., Ren, Z. M. & Moreau, R. Influence of thermoelectric effects on the morphology of Al–Si eutectic during directional solidification under an axial strong magnetic field. *J. Cryst. Growth* **367**, 94–103 (2013).
19. Wang, J. *et al.* Thermoelectric magnetic flows in melt during directional solidification. *Appl. Phys. Letts.* **104**, 121916 (2014).
20. Kaldre, I., Fautrelle, Y., Etay, J., Bojarevics, A. & Buligins, L. Thermoelectric current and magnetic field interaction influence on the structure of directionally solidified Sn–10wt.%Pb alloy. *J. Alloys Comp.* **571**, 50–55 (2013).
21. Wang, J. *et al.* Thermoelectric magnetic force acting on the solid during directional solidification under a static magnetic field. *Appl. Phys. Letts.* **101**, 251904 (2012).
22. Manuwong, T. *et al.* Solidification of Al alloys under electromagnetic pulses and characterization of the 3D microstructures using synchrotron X-ray tomography. *Metal. Mater. Trans. A* **46**, 2908–2915 (2015).
23. Zhang, Y. K., Gao, J. R., Yasuda, H., Kolbe, M. & Wilde, G. Particle size distribution and composition in phase-separated  $\text{Cu}_{75}\text{Co}_{25}$  alloys under various magnetic fields. *Scripta Mater.* **82**, 5–8 (2014).
24. Li, X. *et al.* Investigation of thermoelectric magnetic convection and its effect on solidification structure during directional solidification under a low axial magnetic field. *Acta Mater.* **57**, 2180–2197 (2009).
25. Lehmann, P., Moreau, R., Camel, D. & Bolcato, R. Modification of interdendritic convection in directional solidification by a uniform magnetic field. *Acta Mater.* **46**, 4067–4079 (1998).

26. Wang, J. *et al.* Thermoelectric magnetohydrodynamic flows and their induced change of solid-liquid interface shape in static magnetic field assisted directional solidification. *Metal. Mater. Trans.* **47**, 1169–1179 (2016).
27. Li, D. G., Wang, Q., Liu, T., Li, G. J. & He, J. C. Growth of diffusion layers at liquid Al–solid Cu interface under uniform and gradient high magnetic field conditions. *Mater. Chem. Phys.* **117**, 504–510 (2009).
28. Li, C. J. *et al.* Design and application of differential thermal analysis apparatus in high magnetic fields. *Rev. Sci. Instrum.* **80**, 073907 (2009).
29. Cai, B. *et al.* *In situ* synchrotron tomographic quantification of granular and intragranular deformation during semi-solid compression of an equiaxed dendritic Al–Cu alloy. *Acta Mater.* **76**, 371–380 (2014).
30. Yue, S., Lee, D. P., Poologasundarampillai, G. & Jones, J. R. Evaluation of 3-D bioactive glass scaffolds dissolution in a perfusion flow system with X-ray microtomography. *Acta Biomater.* **7**, 2637–2643 (2011).

### Acknowledgements

This study is partly supported by the Shanghai Committee of Science and Technology (No. 13521101102, 13DZ1108200, 13521101102, 16YF1404300), the program of Youth Eastern Scholar (QD2015035) and CHENGUAN project from Shanghai Municipal Education Commission, and the program of Youth Promotion project from China Association for Science and Technology. The authors greatly appreciate Prof. Thierry Duffar (SiMAP/EPM, Grenoble, France), Prof. Koulis Pericleous and Dr. Andrew Kao (University of Greenwich, UK) for their kind and fruitful discussion.

### Author Contributions

J.W. and Z.M.R. organized the whole experiments and wrote the manuscript, S.Y. and P.D.L. analysed the 3D scanning data, Y.F. helped on the real structure based simulation, and X.L. and Y.B.Z. helped on the experiments.

### Additional Information

**Competing financial interests:** The authors declare no competing financial interests.

**How to cite this article:** Wang, J. *et al.* Refinement and growth enhancement of Al<sub>2</sub>Cu phase during magnetic field assisting directional solidification of hypereutectic Al–Cu alloy. *Sci. Rep.* **6**, 24585; doi: 10.1038/srep24585 (2016).



This work is licensed under a Creative Commons Attribution 4.0 International License. The images or other third party material in this article are included in the article's Creative Commons license, unless indicated otherwise in the credit line; if the material is not included under the Creative Commons license, users will need to obtain permission from the license holder to reproduce the material. To view a copy of this license, visit <http://creativecommons.org/licenses/by/4.0/>